PHOTONICS Research

All-optical manipulation of micrometer-sized metallic particles

YUQUAN ZHANG, XIUJIE DOU, YANMENG DAI, XIANYOU WANG, CHANGJUN MIN, AND XIAOCONG YUAN*

Nanophotonics Research Center, Shenzhen University, Shenzhen 518060, China
**Corresponding author: xcyuan@szu.edu.cn*

Received 12 October 2017; revised 19 November 2017; accepted 24 November 2017; posted 28 November 2017 (Doc. ID 308968); published 16 January 2018

Optical traps use focused laser beams to generate forces on targeted objects ranging in size from nanometers to micrometers. However, for their high coefficients of scattering and absorption, micrometer-sized metallic particles were deemed non-trappable in three dimensions using a single beam. This barrier is now removed. We demonstrate, both in theory and experiment, three-dimensional (3D) dynamic all-optical manipulations of micrometer-sized gold particles under high focusing conditions. The force of gravity is found to balance the positive axial optical force exerted on particles in an inverted optical tweezers system to form two trapping positions along the vertical direction. Both theoretical and experimental results confirm that stable 3D manipulations are achievable for these particles regardless of beam polarization and wavelength. The present work opens up new opportunities for a variety of in-depth research requiring metallic particles.

OCIS codes: (350.4855) Optical tweezers or optical manipulation; (140.7010) Laser trapping; (350.3950) Micro-optics.

https://doi.org/10.1364/PRJ.6.000066

1. INTRODUCTION

Ever since the first demonstration of optical tweezers [1–3], they have attracted extensive academic interest and played a large role in micro-structure trapping [1–7]. The forces exerted on the particles are the origin of the traps. Both experimental and numerical research has been implemented to investigate trapping of dielectric particles [8–11]. Metallic particles are attracting great attention and possess extensive applications in various areas based on their special chemical and physical properties, including spectroscopy, catalysis, micro-fabrication, biotechnology, and medical science [12–15]. The inducements actively promote the development of trapping and manipulation techniques for metallic particles.

Metallic Rayleigh particles ($a \ll \lambda_0$) have been three-dimensionally (3D) trapped by a single laser beam, where scattering forces are small because of the deep-subwavelength particle sizes, and thus easily overcome by gradient forces [16–22]. However, mesoscopic ($a \sim \lambda_0$) and Mie ($a \gg \lambda_0$) metal particles are more challenging to trap optically because the scattering forces are much stronger [23]. The general approach for micrometer-sized (including mesoscopic and Mie sizes) metal particles is to manipulate them in two dimensions by constraining the particles onto a cross section or scanning the laser beam [24,25]. 3D manipulation has already been achieved, but structured light is always employed to form a ring-shaped field to constrain the particle [26–29]. However, a 3D all-optical manipulation using a common single laser beam has not been reported. Consequently, a close look into the key theories and experiments to demonstrate the feasibility of all-optical trapping of micrometer-sized metal particles may provide tantalizing possibilities.

Here, from theory and experiment, we demonstrate a dynamic 3D all-optical manipulation of micro-metallic particles in an inverted optical tweezers system. A numerical analysis of the optical forces was performed using three polarization states (linear, radial, and azimuthal) and three wavelengths (532, 1064, and 1550 nm). For all conditions, the scattered axial force exerted on the particle along the direction of propagation was balanced by the gravitational force at two positions located in front of and behind the focus plane. Furthermore, the simulation results confirm that the traps form regardless of polarization and wavelength, and the experimental results verify perfectly the theoretical expectations. In view of the attractive physical and chemical characteristics of metal materials, such traps open a wider scope for a variety of applications requiring metallic particle manipulation.

2. METHODS AND EXPERIMENTS

To achieve stable 3D all-optical traps, an inverted microscopic system is employed to manipulate the micrometer-sized gold particles, where gravitational forces on the particle play an important role to counteract the optical forces along the direction of propagation. The configuration (Fig. 1) involves a radially polarized laser beam focused by an oil-immersed objective lens

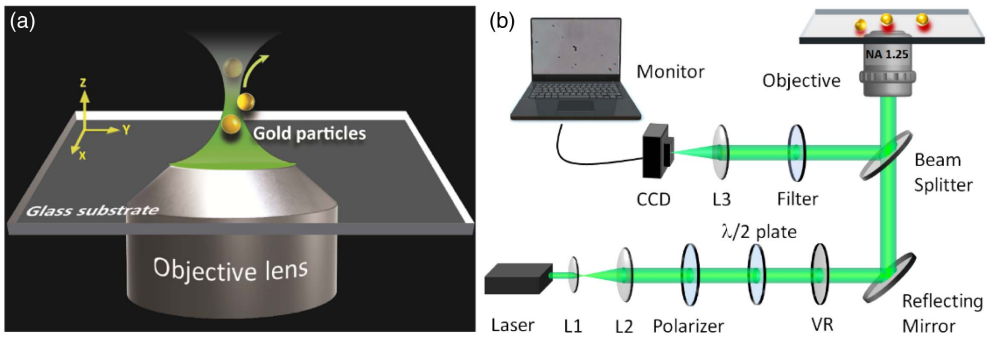

Fig. 1. Schematics of the experimental setup for the all-optical metallic-particle trap. (a) Particles may be trapped at two positions located in front of and behind the focus plane. (b) Detailed experimental setup of the entire system. Gold particle diameters vary from 1.0 to 5.0 μm. L, lens.

with high numerical aperture (NA = 1.25, 100×). Figure 1(a) depicts Au particles manipulated by the all-optical tweezer system. Details of the entire experimental setup are shown in Fig. 1(b). The incident laser beam is first linearly polarized by the polarizer and then expanded through a telescopic system to fit the back aperture of the objective lens. The direction of polarization is controlled by a rotatable half-wave plate, and with a vortex retarder (VR) the polarization is converted to either a radial or azimuthal state. The samples are Au particles (Alfa Aesar Inc.) with diameters from 1.0 to 5.0 μm. A white-light source (not shown) illuminates the samples from above for direct imaging using a CCD camera.

To evaluate the forces underlying the physical processes, many optical models have been proposed and applied. The ray model is popular for micrometer-sized particles, both for dielectric and metal particles [25,26]. For Au particles, more physical and chemical properties need to be considered, e.g., optical absorption. However, the ray model is not always sufficiently precise to analyze the optical forces. Finite-difference time-domain (FDTD) method modeling offers the detail needed for analyzing electrodynamic problems. The electromagnetic distribution strongly influences the optical forces exerted on the particle. Numerical analysis of the electric field distribution around the Au particle with different positions can be performed by a 3D FDTD method. Based on the electric field distribution, Maxwell's stress tensor (MST) is then employed to calculate the forces exerted on the particles [23,30,31]. The time-averaged force acting on a particle is given by the integral of the stress tensor over the surface enclosing the particle. Here, we compute the incident fields using Richards–Wolf vectorial diffraction theory to calculate the tightly focused beams near the focal region of an aplanatic lens, and then implement the scattered field FDTD to evaluate the optical force of the vector beams of interest on metal particles.

3. RESULTS AND DISCUSSION

The total optical force is composed of scattering and gradient components, where the gradient force always opposes the scattering force to form the traps [23]. However, the scattering force is much higher than the gradient force, due to the high absorbing and scattering characteristics of the metal material. In previous work, only the optical forces are taken into account, where the axial optical force is always positive along the direction of propagation to push the particle away [25–27]. However, the gravitational force of the micrometer-sized metallic particle is negligible for it might be of the same order of magnitude as the optical forces. The high scattering force may then be balanced by the sum of gravitational force (including buoyant force) and gradient force. Simulations and experiments were then implemented based on this aspect. Here, taking the gravitational force into consideration, the total force exerted on Au particles was calculated for various sizes and different polarizations and wavelengths of the laser beam. All simulation parameters were chosen consistent with the experimental conditions.

A. Optical Forces Exerted on Au Particles with Different Sizes

In previous work, a 532 nm laser beam was deemed incapable of trapping micrometer-sized Au particles, because of gold's physical characteristics [26]. However, for an inverted microscope system, the gravitational force opposes the axial direction, enabling then the high scattering force to be balanced. Hence, the total force is decomposed into axial and transverse components for further analysis.

Following previous works [26,27], a linearly polarized beam is initially applied in optical manipulations. Figure 2 depicts the axial and transverse forces distributed on Au particles of different sizes. To suppress transverse optical forces acting on the particle, the particle is first located along the axis. The curves in Fig. 2(a) give the resultant axial forces—i.e., optical, gravitational, and buoyancy—acting on the Au particles for various diameters. The vertical optical force is positive because of the high absorbing and scattering characteristics of the Au material, and peaks at the focus and nearby, to accelerate the Au particle. However, the density of Au is very high, and the resultant force of gravity and buoyancy provides an opposing deceleration on the particle. The scattering force is always directed consistently along the direction of propagation, whereas the gradient force points toward the focus. That is, the gradient force is positive in front of the focus but negative behind it. Consequently, two balance positions (crossing points with $F_z = 0$) appear along the axis, in front of and behind the focus plane, indicating the potential for an all-optical trap using a single laser beam for micrometer-sized Au particles.

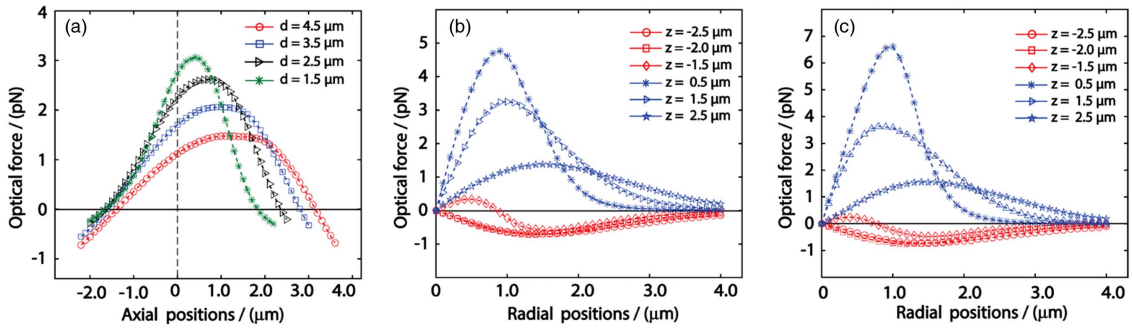

Fig. 2. Forces exerted on gold particles. (a) Axial forces acting on particles of different radii at different points on the optical axis. The focus plane is at $z = 0$. (b), (c) Transverse components of the optical force along the x and y axes, respectively, for various planes along the z-axial direction. Balance ($F = 0$) is achieved at the crossing point of a curve with the abscissa. The gold particle diameter is 2.5 μm in (b) and (c); the 532 nm laser beam is x-directional polarized with a trapping power of 20 mW, in accordance with experimental conditions.

Similarly, Fig. 2(b) plots the transverse component of the force exerted on the gold particles of typical diameters of 2.5 μm, located in different cross sections along the z axis. As the linearly polarized beam produces a non-axisymmetrical field distribution in the focal plane, two typical directions (x and y axes) are calculated to evaluate the transverse trapping efficiency for an x-directional polarized beam. In evidence is a balance reached by the transverse force at the optical axis ($x, y = 0$). Consequently, the particle may be trapped at the two balance positions on the optical axis, where the force reaches equilibrium in the three dimensions.

We also note diverse behaviors in trapping capability of the focused beam for the Au particles outside the focal plane. The forces along the transverse section provide a restoring force pointing toward the axis, when the whole particle is located in front of the focus. However, an opposite effect is seen when the particle moves along the direction of propagation. Intuitively, this is explained by the transverse wave-vector component of the laser beam being directed toward the axis before the focus plane but opposite after the focus. Consequently, although a balance position exists on the axis after the focus, it is not be quite as stable. Furthermore, as the magnitude of optical forces is correlated with the power of the incident laser, the crossing points in Fig. 2(a) could be modulated by varying power of the trapping beam.

B. Dynamic All-Optical Traps of Au Particles

Based on the analysis above, there exist two balance points along the axial direction, where the positive optical force is counteracted by negative force of gravity. With the contribution of transverse forces, particles could be trapped at the position in three dimensions. Figure 3 shows the dynamic behavior of the trapped Au particles in a focused all-optical field (Visualization 1). The trapping source is a linearly polarized 532 nm laser, and the diameter of Au particles varies in the range of 1.0–5.0 μm. A sequence of snapshots extracted from a CCD reveal that a particle located near the focused field can be attracted and trapped at the center and moved along with the laser beam.

As the magnitude of the optical force rises with increased power, the balance is broken when the power is increased; the particle is launched along the direction of propagation.

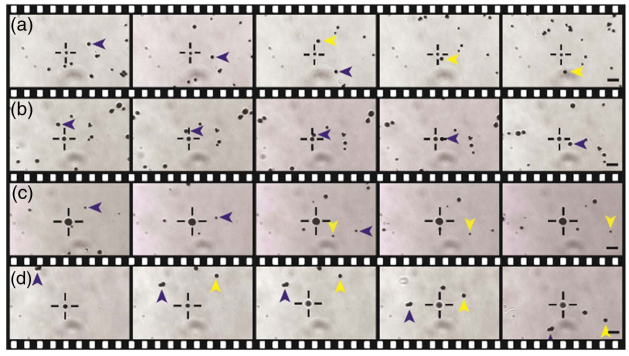

Fig. 3. All-optical manipulation of Au particles of different diameters trapped using a linearly polarized 532 nm laser beam. Black crosses indicate the position of the focused beam; blue and yellow arrows indicate the positions of the reference particles for calibration. Particle diameters range between 1.0 and 5.0 μm: (a) ~1.5 μm, (b) and (d) ~2.5 μm, and (c) ~3.5 μm. The scale bar (black line in lower far-right corner) has length 5.0 μm.

Fortunately, there exists a second balance point behind the focal plane where the particle is recaptured. As this trap is unstable, as discussed above, the manipulation needs to be carefully performed. Such retrieval is also observed in experiments [Fig. 3(d)], but the particle at this second position is obscured as a result of defocusing. The results correlate well with the simulations above and verify the vital contribution that the negative force of gravity makes in trapping.

C. Simulations and Experiments for Different Polarizations and Wavelengths

Here we demonstrate that the optical forces exerted on the metal particles are always positive, regardless of polarization and wavelength. The force of gravity, however, remains negative under all conditions, providing the possibility that all-optical trapping can also be achieved with different polarizations and wavelengths. We numerically explored the variation in force for beams of different polarization configurations. Here, we employed linear, radial, and azimuthal polarizations and beam wavelengths of 532, 1064, and 1550 nm. First, we restricted our approach to situations where the Au particle is

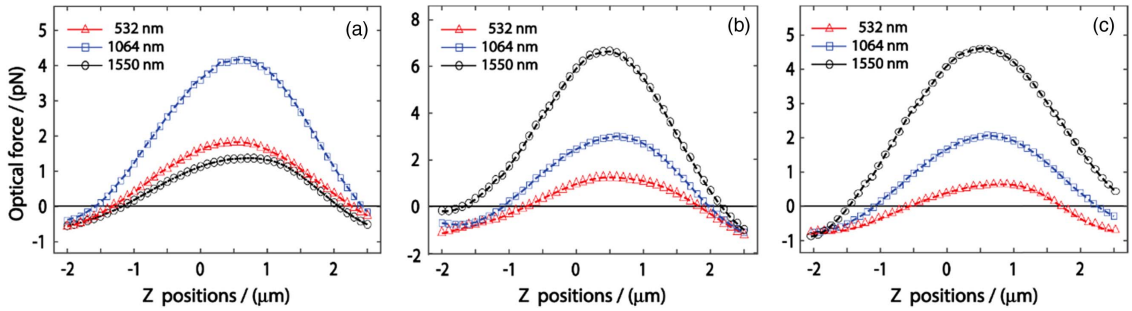

Fig. 4. Axial components of forces exerted on the gold particle (diameter of 2.5 μm) located at the optical axis with (a) linear, (b) radial, and (c) azimuthal polarizations. Beams of wavelengths 532, 1064, and 1550 nm were applied, each with a trapping power of 20 mW.

centrally localized on the optical axis, to reveal possibilities for all-optical trapping. The Au-particle diameter is set at 2.5 μm for all simulations. For each wavelength, three polarizations were calculated; Fig. 4 demonstrates the axial force components exerted on the Au particle. Similar to Fig. 2(a), the resultant axial force includes optical, gravitational, and buoyancy forces. Two balance positions are still in evidence in front of and behind the focal plane. While polarization and wavelength produce slight variations in the trapping position, all-optical trapping is still attainable.

As radial and azimuthal polarizations are axisymmetric, transverse forces were calculated along one diametric direction. Here, a situation where the Au particle is set at different distances from the axis for both polarizations was considered. All other conditions were kept consistent with the above calculations. As crossing points could be modulated by changing power of the trapping beam, the transverse forces at $z = -1.8$ μm are chosen for simulation, to keep consistency with the front balance point in Fig. 2(a) for a 2.5 μm diameter particle. The simulation results (Fig. 5) show that for all wavelengths, the transverse forces provide a restoring force pointing toward the axis in front of the focus. As force at $z = -1.8$ μm is a significant negative value, stable balance is still achievable as he particle moves a little along the axis.

The simulations successfully demonstrated all-optical trapping for all polarization and wavelength settings. From experiments, Fig. 6 shows a sequence of snapshots extracted from a CCD video of a single Au particle trapped using the all-optical tweezer system with different polarizations and wavelengths. The dynamic process can be found in Visualization 2. The particles used had diameters ~2.5 μm, as for simulations. Similarly, two balance positions exist in front of and behind the focus plane; also, in experiments, particles were seen to jump to the latter balance position, when power is increased [Fig. 6(c)].

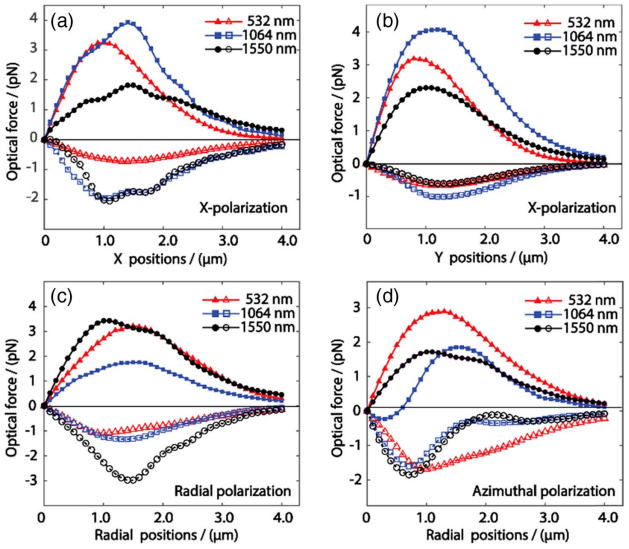

Fig. 5. Transverse components of force exerted on a gold particle (diameter of 2.5 μm) located at the trapping plane in front of the focus with different polarizations and wavelengths. The open symbols and dotted lines represent the forces acting on the particle located at the plane of $z = -1.8$ μm, and the solid symbol and line are those on the plane of $z = 1.5$ μm. Trapping power is 20 mW.

D. Discussion

The analysis and experiments above verified that micrometer-sized metal particles can be trapped at the center of an all-optical field, under high focusing conditions. If the metal particle in the light field is pushed away by the optical force

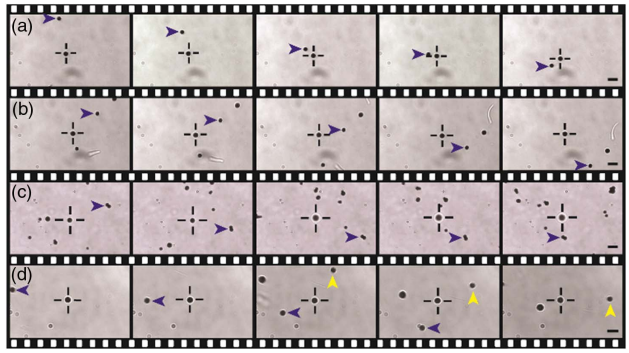

Fig. 6. Dynamic all-optical manipulation of Au particles using beams of different polarizations and wavelengths. (a) Radially polarized 532 nm laser, (b) azimuthally polarized 532 nm laser, (c) radially polarized 1064 nm laser, and (d) linearly polarized 1550 nm laser. A jump is observed in (c). Black crosses indicate the positions of the focused beam, blue and yellow arrows indicate positions of the reference particles for calibration. The Au particles in the experiments have diameter of ~2.5 μm. The scale bar (black line in lower far-right corner) is of length 5 μm.

(calculated using the MST method), the vertical force of gravity pulls the Au particle back. This restoring force is non-negligible for micrometer-sized metal particles. The results indicate that particles can be 3D trapped and manipulated all-optically. In essence, all the traps rely on the presence of gravity to form the optical potential well, providing thus a direct approach in overcoming the barriers to an all-optical manipulation of particles. Furthermore, the trapped particle drops rapidly when the optical field is turned off. The trapping process is notably repeatable, and easy to reestablish once the optical field is returned. Therefore, a stable means for micrometer-sized metal particle manipulation is at hand and has the potential to play a vital role in much research.

4. CONCLUSIONS

We have theoretically, in simulations and experimentally, by using a single laser beam setup, demonstrated stable 3D all-optical trapping of micrometer-sized Au particles ranging from 1.0 to 5.0 μm in diameter. Here, the non-negligible force of gravity plays a vital role in balancing the high repulsive optical forces along the axial direction to form stable traps. The optical forces were calculated by the FDTD and MST methods and were separately analyzed in the transverse and vertical directions. Also, we encountered two trapping positions along the axis located in front of and behind the focal plane. These positions were also observed in experiments and confirmed irrespective of beam polarization and wavelength. This approach removes the prior barriers to 3D all-optical manipulation of micrometer-sized metal particles. It not only provides a simple and effective way for manipulating micrometer sized metallic particles, but also delivers a contribution to reveal the force equilibrium mechanism in optical traps. Furthermore, it provides a convenient potential means to construct particle-based functional structures, e.g., dimers, arrays, or clusters [32–34], for extensive research and applications.

Funding. National Natural Science Foundation of China (NSFC) (91750205, 61377052, 61422506, 61427819, 61605117); National Key Basic Research Program of China (973) (2015CB352004); National Key Research and Development Program of China (2016YFC0102401); Leading Talents of Guangdong Province Program (00201505); Natural Science Foundation of Guangdong Province (2016A030312010, 2016A030310063); Excellent Young Teacher Program of Guangdong Province (YQ2014151).

Acknowledgment. We thank Richard Haase, Ph.D, from Liwen Bianji, Edanz Group China (www.liwenbianji.cn/ac), for editing the English text of a draft of this paper.

REFERENCES

1. A. Ashkin, "Acceleration and trapping of particles by radiation pressure," Phys. Rev. Lett. **24**, 156–159 (1970).
2. A. Ashkin, J. M. Dziedzic, J. E. Bjorkholm, and S. Chu, "Observation of a single-beam gradient force optical trap for dielectric particles," Opt. Lett. **11**, 288–290 (1986).
3. S. Chu, J. E. Bjorkholm, A. Ashkin, and A. Cable, "Experimental observation of optically trapped atoms," Phys. Rev. Lett. **57**, 314–317 (1986).
4. J. R. Moffitt, Y. R. Chemla, S. B. Smith, and C. Bustamante, "Recent advances in optical tweezers," Annu. Rev. Biochem. **77**, 205–228 (2008).
5. M. D. Wang, H. Yin, R. Landick, J. Gelles, and S. M. Block, "Stretching DNA with optical tweezers," Biophys. J. **72**, 1335–1346 (1997).
6. A. Ivinskaya, M. I. Petrov, A. A. Bogdanov, I. Shishkin, P. Ginzburg, and A. S. Shalin, "Plasmon-assisted optical trapping and anti-trapping," Light Sci. Appl. **6**, e16258 (2017).
7. J. Lu, H. Yang, L. Zhou, Y. Yang, S. Luo, Q. Li, and M. Qiu, "Light-induced pulling and pushing by the synergic effect of optical force and photophoretic force," Phys. Rev. Lett. **118**, 043601 (2017).
8. Q. Zhan, "Radiation forces on a dielectric sphere produced by highly focused cylindrical vector beams," J. Opt. A **5**, 229–232 (2003).
9. H. Lu, X. T. Gan, D. Mao, and J. Zhao, "Graphene-supported manipulation of surface plasmon polaritons in metallic nanowaveguides," Photon. Res. **5**, 162 (2017).
10. J. Liu and Z. Li, "Light-driven crystallization of polystyrene microspheres," Photon. Res. **5**, 201 (2017).
11. H. Kawauchi, K. Yonezawa, Y. Kozawa, and S. Sato, "Calculation of optical trapping forces on a dielectric sphere in the ray optics regime produced by a radially polarized laser beam," Opt. Lett. **32**, 1839–1841 (2007).
12. Y. Zhang, J. Shen, Z. Xie, X. Dou, C. Min, T. Lei, J. Liu, S. Zhu, and X. Yuan, "Dynamic plasmonic nano-traps for single molecule surface enhanced Raman scattering," Nanoscale, **9**, 10694–10700 (2017).
13. V. Subramanian, E. E. Wolf, and P. V. Kamat, "Catalysis with TiO_2/gold nanocomposites. Effect of metal particle size on the Fermi level equilibration," J. Am. Chem. Soc. **126**, 4943–4950 (2004).
14. K. Peng, J. Hu, Y. Yan, Y. Wu, H. Fang, Y. Xu, S. T. Lee, and J. Zhu, "Fabrication of single-crystalline silicon nanowires by scratching a silicon surface with catalytic metal particles," Adv. Funct. Mater. **16**, 387–394 (2006).
15. P. K. Jain, X. Huang, I. H. El-Sayed, and M. A. Elsayed, "Noble metals on the nanoscale: optical and photothermal properties and some applications in imaging, sensing, biology, and medicine," Acc. Chem. Res. **41**, 1578–1586 (2008).
16. Q. Zhan, "Trapping metallic Rayleigh particles with radial polarization," Opt. Express **12**, 3377–3382 (2004).
17. P. M. Hansen, V. K. Bhatia, N. Harrit, and L. Oddershede, "Expanding the optical trapping range of gold nanoparticles," Nano Lett. **5**, 1937–1942 (2005).
18. T. Nieminen, N. Heckenberg, and H. Rubinsztein-Dunlop, "Forces in optical tweezers with radially and azimuthally polarized trapping beams," Opt. Lett. **33**, 122–124 (2008).
19. L. Huang, H. Guo, J. Li, L. Ling, B. Feng, and Z. Li, "Optical trapping of gold nanoparticles by cylindrical vector beam," Opt. Lett. **37**, 1694–1696 (2012).
20. L. Bosanac, T. Aabo, P. M. Bendix, and L. B. Oddershede, "Efficient optical trapping and visualization of silver nanoparticles," Nano Lett. **8**, 1486–1491 (2008).
21. F. Hajizadeh and S. N. Reihani, "Optimized optical trapping of gold nanoparticles," Opt. Express **18**, 551–559 (2010).
22. K. Svoboda and S. M. Block, "Optical trapping of metallic Rayleigh particles," Opt. Lett. **19**, 930–932 (1994).
23. C. Min, Z. Shen, J. Shen, Y. Zhang, H. Fang, G. Yuan, L. Du, S. Zhu, T. Lei, and X. Yuan, "Focused plasmonic trapping of metallic particles," Nat. Commun. **4**, 2891 (2013).
24. K. Sasaki, M. Koshioka, H. Misawa, and N. Kitamura, "Optical trapping of a metal particle and a water droplet by a scanning laser beam," Appl. Phys. Lett. **60**, 807–809 (1992).
25. S. Sato, Y. Harada, and Y. Waseda, "Optical trapping of microscopic metal particles," Opt. Lett. **19**, 1807–1809 (1994).
26. M. Gu and D. Morrish, "Three-dimensional trapping of Mie metallic particles by the use of obstructed laser beams," J. Appl. Phys. **91**, 1606–1612 (2002).
27. P. Ke and M. Gu, "Characterization of trapping force on metallic Mie particles," Appl. Opt. **38**, 160–167 (1999).
28. A. T. O'Neil and M. Padgett, "Three-dimensional optical confinement of micron-sized metal particles and the decoupling of the spin and orbital angular momentum within an optical spanner," Opt. Commun. **185**, 139–143 (2000).

29. M. Gu and P. Ke, "Depolarization of evanescent waves scattered by laser-trapped gold particles: effect of particle size," J. Appl. Phys. **88**, 5415–5420 (2000).
30. Y. Zhang, W. Shi, Z. Shen, Z. Man, C. Min, J. Shen, S. Zhu, H. P. Urbach, and X. Yuan, "A plasmonic spanner for metal particle manipulation," Sci. Rep. **5**, 15446 (2015).
31. J. Qin, X. L. Wang, D. Jia, J. Chen, Y. Fan, J. Ding, and H. Wang, "FDTD approach to optical forces of tightly focused vector beams on metal particles," Opt. Express **17**, 8407–8416 (2009).
32. W. Rechberger, A. Hohenau, A. Leitner, J. R. Krenn, B. Lamprecht, and F. R. Aussenegg, "Optical properties of two interacting gold nanoparticles," Opt. Commun. **220**, 137–141 (2003).
33. P. F. Liao and M. B. Stern, "Surface-enhanced Raman scattering on gold and aluminum particle arrays," Opt. Lett. **7**, 483–485 (1982).
34. T. V. W. Janssens, A. Carlsson, A. Puig-Molina, and B. S. Clausen, "Relation between nanoscale Au particle structure and activity for CO oxidation on supported gold catalysts," J. Catal. **240**, 108–113 (2006).